Development 139, 1487-1497 (2012) doi:10.1242/dev.072934

A hindbrain-repressive Wnt3a/Meis3/Tsh1 circuit promotes neuronal differentiation and coordinates tissue maturation

Yaniv M. Elkouby, Hanna Polevoy, Yoni E. Gutkovich, Ariel Michaelov and Dale Frank*

SUMMARY

During development, early inducing programs must later be counterbalanced for coordinated tissue maturation. In *Xenopus laevis* embryos, activation of the Meis3 transcription factor by a mesodermal Wnt3a signal lies at the core of the hindbrain developmental program. We now identify a hindbrain restricting circuit, surprisingly comprising the hindbrain inducers Wnt3a and Meis3, and Tsh1 protein. Functional and biochemical analyses show that upon Tsh1 induction by strong Wnt3a/Meis3 feedback loop activity, the Meis3-Tsh1 transcription complex represses the *Meis3* promoter, allowing cell cycle exit and neuron differentiation. Meis3 protein exhibits a conserved dual-role in hindbrain development, both inducing neural progenitors and maintaining their proliferative state. In this regulatory circuit, the Tsh1 co-repressor controls transcription factor gene expression that modulates cell cycle exit, morphogenesis and differentiation, thus coordinating neural tissue maturation. This newly identified Wnt/Meis/Tsh circuit could play an important role in diverse developmental and disease processes.

KEY WORDS: Meis3, Tsh1, Wnt, Feeback loop, Hindbrain, Neuron differentiation

INTRODUCTION

Early posterior neural development has been extensively studied in vertebrates. BMP antagonism induces neural tissue, whereas posterior specification is driven by caudalizing signaling pathways, such as Wnt/β-catenin, retinoic acid (RA) and FGF (Elkouby and Frank, 2010; White and Schilling, 2008; Dorey and Amaya, 2010). The combined action of these factors induces the midbrain, hindbrain and spinal cord regions. In the anterior, caudalizing antagonists are expressed; a battery of Wnt inhibitors, as well as the RA-degrading enzyme CyP26 (Elkouby and Frank, 2010; White and Schilling, 2008), prevent forebrain caudalization. Much is known about neural caudalization and its antagonism in the anterior, but little is known about the intrinsic negative regulatory pathways that act within the posterior neural tissue. Negative regulation within the hindbrain and spinal cord domains could regulate the transition of induced proliferating progenitor populations to differentiation, thus controlling cell number, cell fate, tissue size, morphology and function.

In early *Xenopus* and zebrafish development, the Meis3 TALE-family transcription factor induces the hindbrain, including primary neurons and neural crest (Dibner et al., 2001; Vlachakis et al., 2001; Waskiewicz et al., 2001; Gutkovich et al., 2010). Hindbrain induction by a mesodermal Wnt ligand is a conserved vertebrate feature, and mesodermal Wnt3a directly activates neural *Meis3* expression to trigger the hindbrain developmental program, regulating expression of Hox paralogous group 1-4 genes (Dibner et al., 2004; Elkouby et al., 2010).

Wnt3a is also expressed in the neural plate (McGrew et al., 1997), but a thorough investigation of later neural Wnt3a function in the hindbrain is lacking. We now show that early hindbrain-inducing components act later to repress the hindbrain developmental program. Contrasting early mesodermal Wnt3a activity, later neural Wnt3a plays a negative role in hindbrain development. Neural Wnt3a and Meis3 proteins act by a positive-feedback mechanism. The resulting accumulation of Meis3 protein above a threshold level triggers auto-repression of *Meis3* gene expression. At high levels, Meis3 induces expression of the co-repressor protein, *Teashirt1* (*Tsh1*). Initially, Meis3 protein directly activates its own gene expression; later, Tsh1 is recruited to the *Meis3* promoter by Meis3 protein to repress transcription. In the hindbrain, Tsh1 protein acts as a switch, shifting the cellular response to the Wnt signal from activation to repression of *Meis3* gene expression. We further show that Meis3 protein plays a dual role in the hindbrain, both inducing neural progenitors and maintaining their proliferative state. The role of the repressive Wnt/Meis/Tsh circuit is to restrain Meis3 protein to levels that enable cell cycle exit and neuron differentiation. In this circuit, Tsh1 protein coordinates neural tissue maturation. This newly identified Wnt/Meis/Tsh circuit could have an important role in regulating a diverse range of developmental and disease processes.

MATERIALS AND METHODS

Xenopus embryos

Ovulation, in vitro fertilization, embryo culture, dissections and explant culture were as described previously (Re'em-Kalma et al., 1995; Bonstein et al., 1998).

Plasmid constructs

Meis3-HA

The HA tag fragment was cut (*Cla*I/*Eco*RI) from a pcDNA3 plasmid (*Cla*I/*Eco*RI). A Meis3 full-length fragment was cut (*Eco*RI/*Not*I) from pCS107 and subcloned into pGEM T-Easy. The HA tag was subcloned into pGEM-T Easy-Meis3 (*Cla*I/*Eco*RI). The HA-Meis3 was then cut (*Cla*I/*Not*I) and subcloned back into the pCS107 vector.

*Meis*3 5′UTR probe plasmid

A fragment of the *Meis3* 5′UTR was PCR amplified by *Meis3UTR* primers (supplementary material Table S1), from a pGL3 plasmid containing *Meis3* 5′ genomic sequence, the entire 5′UTR, the 1st exon and part of the 1st intron (Elkouby et al., 2010). The *Meis3* 5′UTR fragment was cloned into pGEM-T Easy.

Department of Biochemistry, The Rappaport Family Institute for Research in the Medical Sciences, Faculty of Medicine, Technion-Israel Institute of Technology, Haifa 31096, Israel.

*Author for correspondence (dale@tx.technion.ac.il)

Accepted 16 February 2012

RNA, DNA and morpholino oligonucleotide (MO) injections

Capped sense in vitro transcribed full-length mRNA, *BMPR1A dominant-negative receptor* (*DNR*), *Meis3* (Salzberg et al., 1999), *Meis-Myc*, *VP16-Meis3* (Dibner et al., 2001), *Meis3-GR* (Dibner et al., 2004), *Tsh1*, *Myc-Tsh1* (Koebernick et al., 2006), *Dkk1* (Glinka et al., 1998) and *THVGR* (Wu et al., 2005) were injected into one-cell embryos. *Xenopus Wnt3a* (pCS107) plasmid (Elkouby et al., 2010) was also injected in CMV-driven zygotic expression assays. MOs (Gene Tools) used were *Meis3*-MO (Dibner et al., 2001), *Wnt3a*-MO (Elkouby et al., 2010) and *Tsh1*-MO (Koebernick et al., 2006).

In situ hybridization

Whole-mount in situ hybridization was performed with digoxigenin-labeled probes (Harland, 1991) *Meis3, EphA2* (Dibner et al., 2001), *Wnt3a* (Fonar et al., 2011), *N-Tubulin* (*N-Tub*), *Slug* (Gutkovich et al., 2010), *Tsh1* (Koebernick et al., 2006), *Iro3* (Gomez-Skarmeta et al., 1998) and *Sox3* (Hardcastle and Papalopulu, 2000).

Semi-quantitative (sq) RT-PCR analysis

sqRT-PCR was performed (Snir et al., 2006). In all sqRT-PCR experiments, three to six independent experiment repeats were typically performed. In all experiments, each sample was routinely assayed a minimum of two times for each marker. See supplementary material Table S1 for primer sequences.

Chromatin immunoprecipitation (ChIP)

One-cell embryos were injected with *Meis3-Myc* (0.8 ng) (Dibner et al., 2001) or *Myc-Tsh1* (0.5 ng) (Koebernick et al., 2006) encoding RNAs and/or the *Meis3*-MO (30 ng). For each group, ~30 stage 17 embryos were crosslinked by 1% formaldehyde/PBS for 35 minutes. Crosslinking was quenched by 0.125 M glycine/PBS, followed by three washes in PBS and freezing at –80°C. ChIP was performed with either rabbit IgG (control; Pierce) or anti-Myc antibody (rabbit polyclonal, Millipore) as described previously (Blythe et al., 2009; Elkouby et al., 2010), except that DNA shearing was performed by Bioruptor sonicator (Diagenode) for 11 cycles of 30 seconds ON, 30 seconds OFF on high power output, and after immunoprecipitation, beads were washed five times in wash buffer I (Blythe et al., 2009) and once in TE prior to elution. Quantitative PCR (QPCR) was performed using a Stratagene Mx3000P device and SYBR Premix Ex Taq II (Takara). QPCR conditions were: 2 minutes at 95°C (initial melting), the 50 cycles of 15 seconds at 95ºC and 1 minute at 60ºC, followed by a melting curve gradient. For all primers, concentrations and threshold values were carefully calibrated to consistently provide linear reaction over five orders of magnitude, with an ideal slope of –3.322±0.1. For all ChIP experiments, a minimum of three independent repeats were performed; each sample was analyzed by QPCR in duplicate. See supplementary material Table S2 for amplicon data and primer sequences.

Co-immunoprecipitation (Co-IP)

Meis3-HA (cold Met), Myc-Tsh1 (S^{35}Met) and Cyp26 (S^{35}Met) were in vitro translated (Promega, TNT SP6 Quick Coupled Transcription/Translation System). Proteins were mixed in [20 mM HEPES (pH 7.9), 100 mM NaCl, 1 mM DTT, 6 mM $MgCl_2$, 1% NP-40, 0.5 mM EDTA, 20% glycerol] and incubated for 1 hour at room temperature with nutation. An input sample was set aside and the remaining mix was immunoprecipitated by pre-cleared blocked protein-G agarose beads (Invitrogen), with either IgG (control; Invitrogen) or anti-HA antibody (Pierce). Beads were washed five times in the above buffer and proteins were eluted. Immunoprecipitation and input samples were run on 10% SDS-PAGE gels.

Western blot and immunohistochemistry

Western blot analysis was performed as described previously (Dibner et al., 2001). Immunostaining was performed as described previously (Aamar and Frank, 2004) with a phospho Histone H3 antibody (Ser10; Upstate) on whole neural tubes that were dissected from embryos just prior to fixation. For photographic analysis, neural tubes were transferred to 2:1 benzyl benzoate:benzyl alcohol for clearing. For each neural tube, images of 25 different focal planes were stacked in order to visualize proliferating cells efficiently across the tissue. In three independent experiments, approximately 30 neural tubes were analyzed in each group.

Dispersed ectodermal explants

Intact animal caps (ACs) were removed at blastula stage 8-9 and cultured in low calcium magnesium Ringer's medium (LCMR). In parallel, ACs were dispersed and cultured in calcium- and magnesium-free medium (CMFM). Cells were dispersed by gentle pipetting and swirling; intact and dispersed ACs were cultured on agarose coated-plates until neurula stages. Dispersed cells were concentrated in Eppendorf tubes by gentle centrifugation in CMFM at 1000 ***g*** for 1 minute. RNA was isolated for sqRT-PCR as described from 18 intact explants and 36 dispersed explants. In all experiments, epidermal cytokeratin expression was compared between intact and dispersed ACs. Efficient dispersal prevents BMP signaling in the AC explants, which strongly reduces epidermal cytokeratin expression. In all dispersal experiments, expression of epidermal cytokeratin was not detected in dispersed versus intact AC explants (not shown).

RESULTS

Meis3 and Wnt3a act in a negative-feedback loop within the neural plate

In *Xenopus*, a mesodermal-derived Wnt3a signal induces the hindbrain at mid-gastrula stages (Elkouby et al., 2010), yet the later role of neural-specific Wnt3a in this process is unknown. We examined Meis3 and Wnt3a activity interactions at later neural plate stages. *Meis3*-deficient embryos do not express *Wnt3a* in the neural plate at late-gastrula nor mid-neurula stages (Fig. 1Ab,e), whereas *Wnt3a* expression is robustly expanded in embryos over-expressing Meis3 protein (Fig. 1Ac,f). Meis3 is necessary and sufficient for both the onset and maintenance of *Wnt3a* expression in the neural plate (Fig. 1Ag). Cyclohexamide (CHX) assays in animal cap (AC) explants suggest that Meis3-mediated regulation of *Wnt3a* expression is direct (not shown). Thus, early mesodermal Wnt3a induces neural *Meis3* expression and Meis3 protein activates later *Wnt3a* expression in the neural plate.

We examined the effects of ectopic Wnt3a activity on *Meis3* expression at later neurula stages. *Meis3* expression is activated at gastrula stages by the inducible constitutively active Tcf protein (THVGR; Fig. 1Bb) (Elkouby et al., 2010), but at later stages THVGR suppresses *Meis3* expression (Fig. 1Be). This phenomenon is *Meis3* specific, as expression of other regional neural markers, such as *En2* (isthmus) and *EphA2* (r4) is clearly detected (Fig. 1Bi); the hindbrain region has formed, but it no longer expresses *Meis3*. In this experiment, THVGR robustly induced expanded *Meis3* expression at gastrula stages (Fig. 1Bb). Wnt3a caudalizing activity is strictly Meis3 dependent (Elkouby et al., 2010), so in these experiments the early increase in Meis3 protein caudalized the neural plate, as *En2* and *EphA2* expression is expanded anteriorly (Fig. 1Bi). Only later does this ectopic Wnt activity repress *Meis3* expression (Fig. 1Be). Like THVGR, zygotic-driven *Wnt3a* overexpression also represses later *Meis3* expression (Fig. 2Bb). These results suggest that *Meis3* repression by Wnt3a/β-catenin is part of a hindbrain negative-feedback loop.

We determined the timing of this shift in *Meis3* transcriptional response to Wnt/β-catenin activity. Similar to gastrula stages (Fig. 1Bb), mid-neurula stage THVGR activation also suppressed later *Meis3* expression (Fig. 1Bf), but contrastingly, this later THVGR activation cannot caudalize; *En2* and *EphA2* expression is unaffected (Fig. 1Bj). Unactivated THVGR does not affect *Meis3* expression or neural caudalization (insets of Fig. 1Bf,j). Consistent with negative-feedback activity, Wnt/β-catenin signaling suppresses *Meis3* expression only after hindbrain induction (Fig. 1Bk). Reciprocally, overexpression of the zygotic Wnt antagonist *Dkk1* eliminates *Meis3* expression at gastrula stages (Elkouby et al., 2010; Fig. 1Bc), but at later-neurula stages, *Meis3* expression

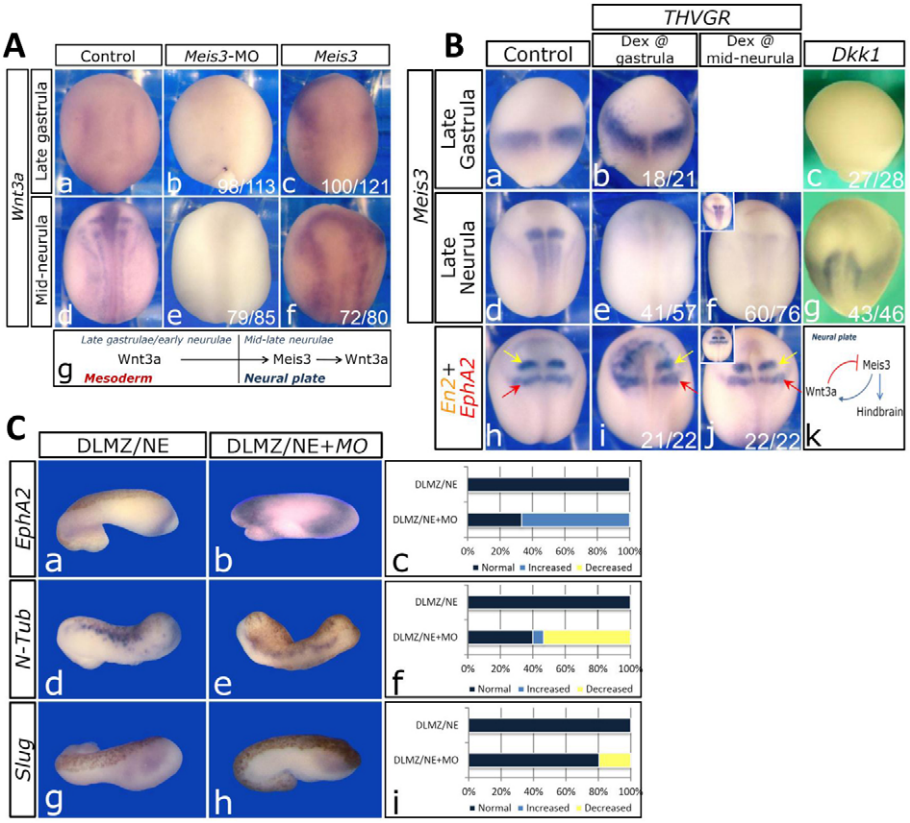

Fig. 1. A neural Wnt3a-Meis3 loop restricts hindbrain development. (**A**) *Wnt3a* expression in late-gastrula (a-c) or mid-neurula (d-f) embryos injected at the one-cell stage with either *Meis3*-MO (25 ng) or *Meis3* mRNA (0.5 ng). In all figures, the phenotype frequency is indicated in each panel. (g) A schematic summary of the results. (**B**) *Meis3* expression in late-gastrula (a-c) or mid-neurula (d-g) stage embryos injected at the one-cell stage with either *THVGR* (50 pg) or *Dkk1* (35 pg) mRNAs. THVGR was activated by 1 μM dexamethasone (Dex) at gastrula (b,e,i) or mid-neurula (f,j) stages. Unactivated THVGR controls develop normally (insets in f, j). (k) A schematic summary of the results. See supplementary material Fig. S1. (**C**) *EphA2* (a,b), *n-Tub* (d,c) and *Slug* (g,h) expression in mid-neurula stage DLMZ/NE recombinant explants (see text). For each recombinant: DLMZ is the pigmented-brownish tissue on the left/top (except in b, where it is on the back of the explant); NE is the albino tissue on the right/bottom. NEs are from embryos injected with BMP dominant-negative receptor (DNR) mRNA (160pg) and/or *Wnt3a*-MO (40ng). (c,f,i) The expression phenotype for pooled explants; for each group, 14-16 explants were examined per marker.

is restored to fairly high levels (Fig. 1Bg). We also show that this *Meis3* repression is dependent on Meis3-induced, neural Wnt3a activity (supplementary material Fig. S1A,B).

Our previous experiments showed that Meis3 induced by mesodermal Wnt3a protein caudalizes neural cell fates and rescues posterior neural cell fates in Wnt-deficient embryos (Elkouby et al., 2010). These results suggest that neural-specific Wnt3a does not act downstream to Meis3 to caudalize. Alternatively, neural-Wnt3a activity may control a negative-feedback loop that represses later *Meis3* expression, optimizing Meis3 protein levels in the neural plate.

To elucidate neural Wnt3a function, we performed recombinant explant assays. Dorsolateral marginal zone (DLMZ) explants induce posterior neural cell fates in adjacently recombined neural ectoderm (NE) via secretion of Wnt3a (Elkouby et al., 2010). We now performed these experiments by recombining wild-type (WT) DLMZs with Wnt3a-deficient NE explants (Fig. 1C). The DLMZ robustly induced posterior neural marker expression in Wnt3a-deficient NE. Moreover, expression of the *EphA2* hindbrain (r4) marker was not inhibited, but dramatically expanded in nearly 70% of the explants (Fig. 1Ca-c), suggesting a hindbrain inhibitory role for neural-specific Wnt3a protein. Expression of *N-Tub* (differentiated primary neurons) was fairly normal in 40% of the explants (Fig. 1Cd-f). However, 60% of the explants showed either a strong increase or a moderate decrease in expression, implying a later Wnt3a modulation of neuron differentiation (Fig. 1Cd-f). Expression of *Slug* (neural crest) was not affected in 80% of the explants (Fig. 1Cg-i). These results suggest that neural-specific Wnt3a is not required for neural caudalization per se, but plays a role to fine-tune cell fate distribution. Furthermore, by mid-neurula stages, neural tissue has already lost its competence to Wnt/β-catenin caudalizing activity (Fig. 1Bj). Further elucidating this point, in isolated and recombinant AC explants, Meis3 induction of hindbrain markers such as *EphA2*, *Krox20*, *HoxA2* and *Gbx2* and *HoxB3* is not inhibited, but even somewhat stimulated by simultaneous disruption of Wnt activity, whereas the spinal cord marker *HoxB9* was inhibited (supplementary material Fig. S1C-E). Supporting this observation that later Wnt-signaling represses hindbrain fates, Meis3 rescue of Dkk1-injected/Wnt-depleted embryos consistently led to highly ectopically disorganized *Krox20* and *EphA2* expression levels (Elkouby et al., 2010). Although mesodermal Wnt3a drives the hindbrain developmental program, neural-expressed Wnt3a could play a negative regulatory role in the neural plate. As Wnt3a is traditionally considered a strong neural caudalizer, we addressed its potential counterintuitive negative regulatory role in the hindbrain.

Repression of *Meis3* gene expression by Wnt3a/β-catenin is mediated by Meis3 protein

Given the importance of Meis3 protein in hindbrain development, we investigated its repression mechanism. We overexpressed *Meis3* about twofold higher than the typical overexpression concentration that caudalizes embryos. These higher Meis3 levels repress endogenous *Meis3* gene expression as detected by a *Meis3 5′UTR* probe that specifically recognizes endogenous, but not exogenously injected *Meis3* mRNA (Fig. 2Aa,b). As a control, a *Meis3 ORF* probe detects the ectopically injected *Meis3* mRNA (Fig. 2Ac,d). Ectopic Meis3 levels repress endogenous *Meis3* expression at high Meis3 levels (Fig. 3G), suggesting that Meis3 protein must accumulate over a concentration threshold to initiate auto-repression. Accumulation of Meis3 protein in the neural tissue of normal embryos probably controls the exact timing of endogenous auto-repression. Indeed, at mid-neurula stages, when THVGR suppresses *Meis3* expression, *Meis3* is already expressed at high levels (Fig. 1Ba,d).

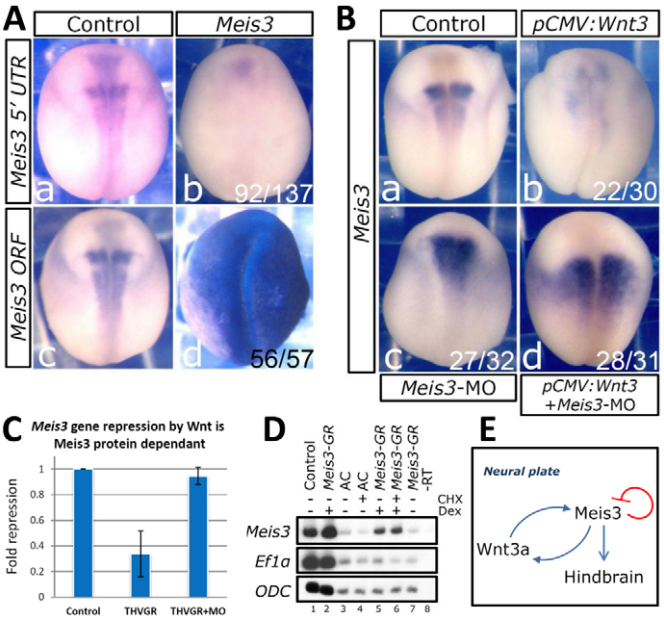

Fig. 2. Wnt3a represses *Meis3* expression via auto-regulation by Meis3 protein. (**A**) *Meis3-5′UTR* (a,b) and *Meis3-ORF* (c,d) expression in mid-neurula embryos injected at the one-cell stage with high levels of *Meis3* mRNA (1 ng). (**B**) *Meis3-5′UTR* expression in mid-neurula embryos injected at the one-cell stage with *Wnt3* CMV-driving plasmid (60 pg; *pCMV:Wnt3*; b) or *Meis3*-MO (30 ng; c), or both (d). (**C**) RT-PCR to endogenous *Meis3 (Meis3-5′UTR* primers) in AC explants from embryos injected with *THVGR* mRNA (50 pg) or *Meis3*-MO (30 ng), or both. RNA was isolated from a pool of 18 mid-neurula explants in each group. Results were quantified, normalized to *Ef1α* loading control and plotted as fold-repression. Bars are s.e.m. from three independent experiments. (**D**) CHX assay and RT-PCR in embryos (lanes 1-2) and AC explants (lanes 3-7) injected with *Meis3-GR* mRNA (250 pg). At early gastrula stages, 5 μM CHX was added to explant medium 2 hours prior to Dex activation (1 μM). Explants were analyzed at late gastrula stages. Unactivated Meis3-GR shows no leaky activity. *Ef1α* is a positive control for CHX activity, *ODC* is a loading control. –RT samples showed no DNA contamination. (**E**) A schematic summary of the results.

We next examined the epistatic relationship between Wnt3a/β-catenin and Meis3 activities in the context of Meis3 repression. Similar to THVGR overexpression, zygotic Wnt3a overexpression strongly represses *Meis3* expression (Fig. 2Bb). Further confirming Meis3 auto-repression, endogenous *Meis3* expression is expanded in *Meis3*-deficient embryos (Fig. 2Bc). Wnt3a overexpression in *Meis3*-deficient embryos, however, cannot repress *Meis3* gene expression; this combination of activating an inducer while withdrawing a repressor, strongly expands *Meis3* expression (Fig. 2Bd). This upregulated expanded pattern strikingly mimics the earlier, broader, *Meis3* expression pattern seen in late-gastrula stages. We validated these results by overexpressing THVGR in wild-type versus Meis3-deficient AC explants. THVGR reduction of basal *Meis3* expression in ACs is Meis3 dependent (Fig. 2C). Apparently, Meis3 represses its own expression more directly, whereas Wnt3a/β-catenin activates *Meis3* gene expression, probably increasing cellular Meis3 protein levels above the threshold level required for auto-repression (Fig. 2E). Indeed, CHX assays in AC explants suggest that the *Meis3* gene is a direct-target of the Meis3 protein (Fig. 2D), and this early positive auto-regulation was also observed in vivo (supplementary material Fig. S2).

Tsh1 protein is a repressor of *Meis3*

Meis family proteins typically act as transcriptional activators (Dibner et al., 2001; Inbal et al., 2001). Thus, Meis3 autorepression activity may require interactions with transcription repressor partners. During *Drosophila* development, Tsh and Hth (Meis) proteins interact to repress gene expression (Casares and Mann, 2000; Bessa et al., 2002). In *Drosophila* gut development, *Tsh* expression is induced by high Wg levels, and Tsh protein then acts to repress Wg target gene expression (Waltzer et al., 2001). In the hindbrain, Tsh proteins could act to restrain the Wnt/β-catenin response, fitting the *Meis3* repression scenario we observe. In *Xenopus* hindbrain development, both Tsh1 gain and loss of function inhibit expression of hindbrain markers (Koebernick et al., 2006), suggesting a negative-feedback effect. Tsh1 protein is thus a good candidate for interacting with Meis3 to mediate its auto-repression.

Ectopic Tsh1 levels indeed repress *Meis3* expression in neurula embryos (Fig. 3A). In *Tsh1*-deficient embryos, *Meis3* expression is upregulated and expanded. This expanded expression pattern strikingly resembles the normal broader *Meis3* pattern seen in late gastrula and early neurula stages (Fig. 3Cc and inset). For Tsh1 deficiency, we used the *Tsh1*-MO that specifically knocks-down Tsh1 protein (Koebernick et al., 2006). Verifying *Tsh1*-MO specificity in our system, *Tsh1* mRNA overexpression restores the normal *Meis3* expression pattern in Tsh1-morphant embryos (supplementary material Fig. S3A). Thus, Tsh1 protein is an endogenous repressor of *Meis3* gene expression. Indeed, *Tsh1* and *Meis3* transcripts overlap in the hindbrain (supplementary material Fig. S3B). Tsh1 protein probably represses the *Meis3* gene cell autonomously, as ectopic Tsh1 protein sharply inhibits *Meis3* expression levels in dissociated AC explants (supplementary material Fig. S3C).

Tsh1 transcripts are absent in gastrulae; zygotic expression only initiates at early neurula stages (Koebernick et al., 2006). These expression dynamics correlate with the negative shift in *Meis3* transcriptional response to Wnt/β-catenin. Tsh1 protein could serve as a switch, in which Tsh1-negative cells continue to upregulate *Meis3* in response to Wnt3a/β-catenin, whereas Tsh1-positive cells suppress *Meis3* expression. Wnt/β-catenin activity in Tsh1-negative hindbrain cells of gastrula to early neurula stages upregulates *Meis3* expression (Fig. 1Ba,b), while the same activity in Tsh1-positive hindbrain cells of mid-neurula onwards stages downregulates it (Fig. 1Bd-f). To test whether Tsh1 serves as a switch, *Meis3* expression was examined in Tsh1 overexpressing embryos at mid- and late-gastrula stages, when Wnt3a/β-catenin activates *Meis3* expression, but before endogenous Tsh1 protein is expressed (Koebernick et al., 2006). Indeed, precocious ectopic Tsh1 levels repress *Meis3* expression (Fig. 3B).

We determined that later *Meis3* repression by Wnt3a/β-catenin is indeed Tsh1 dependent. THVGR strongly represses *Meis3* expression (Fig. 3Cb), and in Tsh1-deficient embryos *Meis3* expression is significantly expanded (Fig. 3Cc). Strikingly, in Tsh1-deficient embryos, THVGR continues to robustly induce and expand *Meis3* expression (Fig. 3Cd), mimicking its early *Meis3* inducing activity (Fig. 3Cd, inset). Therefore, in Tsh1-negative cells, Wnt3a/β-catenin signaling perpetuates *Meis3* expression, failing to shift to the later repression program. Tsh1 switches the cellular response of the Wnt3a/β-catenin signal from activation (Fig. 3Cd′) to repression (Fig. 3Cb′) of *Meis3* gene expression.

Tsh1 expression is regulated by Meis3

Tsh1 expression dynamics and the threshold levels of Meis3 activity required to repress *Meis3* expression suggest that *Tsh1* expression initiation at neurula stages is regulated by Meis3 and

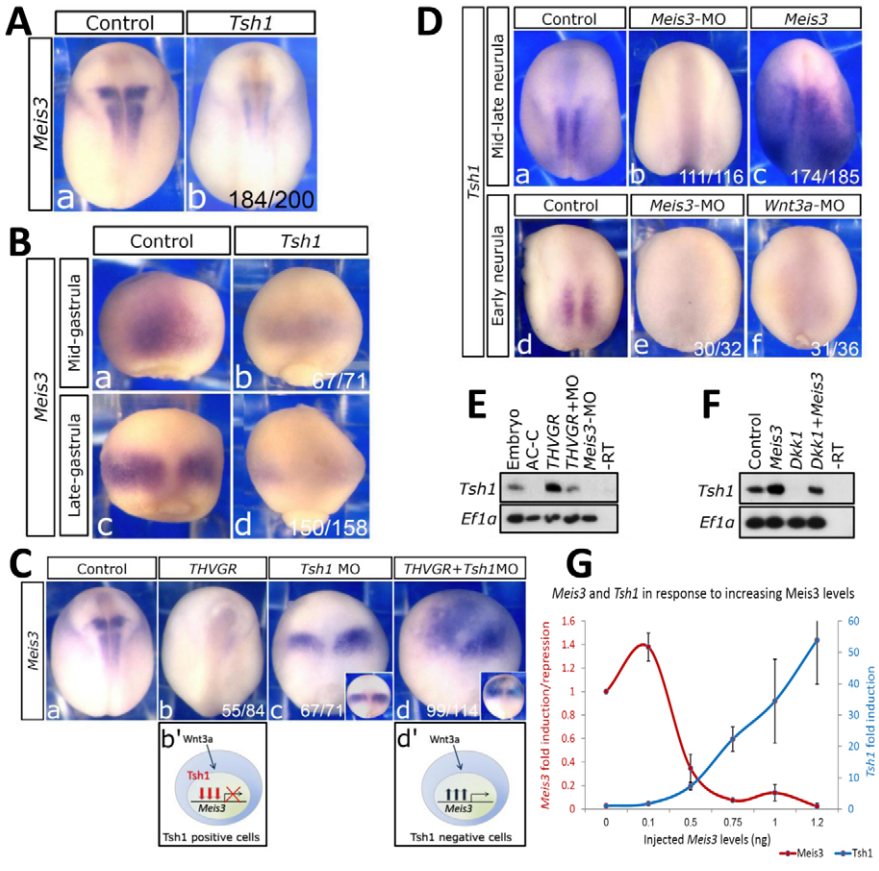

Fig. 3. Tsh1 is a *Meis3* gene repressor that modulates Wnt/β-catenin activity and is regulated by Meis3 protein. (**A**,**B**) *Meis3* expression in (Aa,b) mid-neurula and (Ba-d) gastrula embryos injected at the one-cell stage with *Tsh1* mRNA (0.5 ng). (**C**) *Meis3* expression in mid-neurula embryos injected at the one-cell stage with *THVGR* mRNA (40 pg; b) or *Tsh1*-MO (5 pmol; c), or both (d). Insets in c, d show *Meis3* expression in late gastrula wild-type or *THVGR*-injected embryos, respectively. b′ and d′ schematically show Tsh1 modulation of the Wnt/β-catenin transcriptional response of *Meis3*. (**D**) *Tsh1* expression in mid or early-neurula embryos injected at the one-cell stage with *Meis3*-MO (30 ng; b,e) or *Meis3* mRNA (1 ng; c), or the *Wnt3a*-MO (45 ng; f). (**E**) RT-PCR to *Tsh1* in mid-neurula stage AC explants from embryos injected with *THVGR* mRNA (40 pg) or *Meis3*-MO (30ng), or both. (**F**) RT-PCR to *Tsh1* in mid-neurula embryos injected with *Meis3* mRNA (0.8 ng) or *Dkk1* mRNA (35 pg), or both. (**G**) Transcriptional kinetics of *Tsh1* and *Meis3* genes in response to increasing levels of Meis3 protein. RT-PCR was performed on pools of 18 mid-neurula AC explants from embryos injected with *Meis3* mRNA (0.1-1.2ng). Results were quantitated and normalized to the *Ef1α* control, and plotted as fold change. Bars are s.e.m. from three independent experiments. –RT samples showed no DNA contamination. A '0' *x*-value is a non-injected control, with a '1' *y*-value as a basal expression level.

Wnt3a/β-catenin. *Tsh1* expression is eliminated in Meis3-deficient mid-late neurula stage embryos (Fig. 3Db), and induced and expanded in *Meis3* overexpressing embryos (Fig. 3Dc). Meis3 is both necessary and sufficient for *Tsh1* gene expression. At early neurula stages, either Meis3 or Wnt3a proteins are required for the induction of *Tsh1* expression (Fig. 3De,f). We concluded that Wnt3a/Meis3 epistasis controls *Tsh1* expression. THVGR induction of *Tsh1* expression in AC explants is Meis3 dependent (Fig. 3E) and Meis3 rescues *Tsh1* expression in *Dkk1* overexpressing embryos (Fig. 3F). Consistent with Meis3 protein being directly required for *Meis3* gene repression, it also acts downstream of Wnt3a/β-catenin to regulate *Tsh1* expression. Activation of *Tsh1* expression by Meis3 activity may not necessarily be cell autonomous (not shown) and may require additional non-autonomous Wnt activity. Whereas Meis3 rescues *Tsh1* expression to control levels in Dkk1 embryos, Meis3 alone induces more robust *Tsh1* expression (Fig. 3F). Meis3 seems to serve as the limiting factor, but Wnt activity may also contribute to *Tsh1* expression. Furthermore, we measured *Meis3* and *Tsh1* expression in response to Meis3 activity. There was a strong correlation between *Meis3* repression and *Tsh1* induction; only high Meis3 levels that induce *Tsh1* can repress *Meis3* expression (Fig. 3G). Lower Meis3 levels neither induce *Tsh1* nor repress *Meis3* expression (Fig. 3G). These lower Meis3 levels still caudalize, as they strongly induce expression of the Meis3-responsive hindbrain marker *Krox20* (not shown). Thus, induction of *Tsh1* expression requires high levels of Meis3 activity. In this scenario, Wnt3a/β-catenin activity induces Meis3 levels over a critical cellular threshold; Meis3 activates *Tsh1* expression, which then represses *Meis3* gene expression.

Meis3 and Tsh1 proteins act in a complex to repress *Meis3* gene expression directly

As Wnt3a/β-catenin repression of *Meis3* expression is dependent on both Meis3 and Tsh1 proteins, we examined epistasis between these two proteins. We monitored repression of *Meis3* expression by overexpressing one protein while simultaneously knocking down the other. Each of these proteins is sufficient to strongly repress *Meis3* expression (Fig. 4A,B), but they mutually require the activity of one another to do so. Neither overexpression of Meis3 on a Tsh1-deficient background, nor reciprocal overexpression of Tsh1 on Meis3-deficient background represses *Meis3* expression (Fig. 4Ac,Bc). These embryos more closely resembled the Tsh1- or Meis3-deficient phenotypes, respectively (Fig. 4Ad,Bd). Moreover, the combined knock down of these proteins synergistically expands *Meis3* expression to its broader earlier-like pattern (supplementary material Fig. S4). Therefore, Meis3 and Tsh1 are not epistatic to one another, but jointly act to repress *Meis3* expression.

We previously identified a 3 kb region of the *Xenopus laevis Meis3* promoter that drives *Meis3*-like, hindbrain-specific, reporter gene expression in transgenic animals (Elkouby et al., 2010). We examined whether Meis3-Tsh1 proteins could directly repress *Meis3* expression on the *Meis3* promoter. There are two putative Meis consensus binding sites in the *Xenopus laevis Meis3* promoter region: MeisA, –486 bp upstream to the transcription start site; MeisB, +356 bp downstream, in the 5′UTR (Fig. 4C). By in vivo ChIP analysis, we determined whether these sites bound Meis3 protein at mid-late neurula stages in *Meis3-Myc*-expressing embryos. Both the *MeisA* and *MeisB* sites were specifically enriched in the Meis3-IP sample, and not in the IgG-IP control

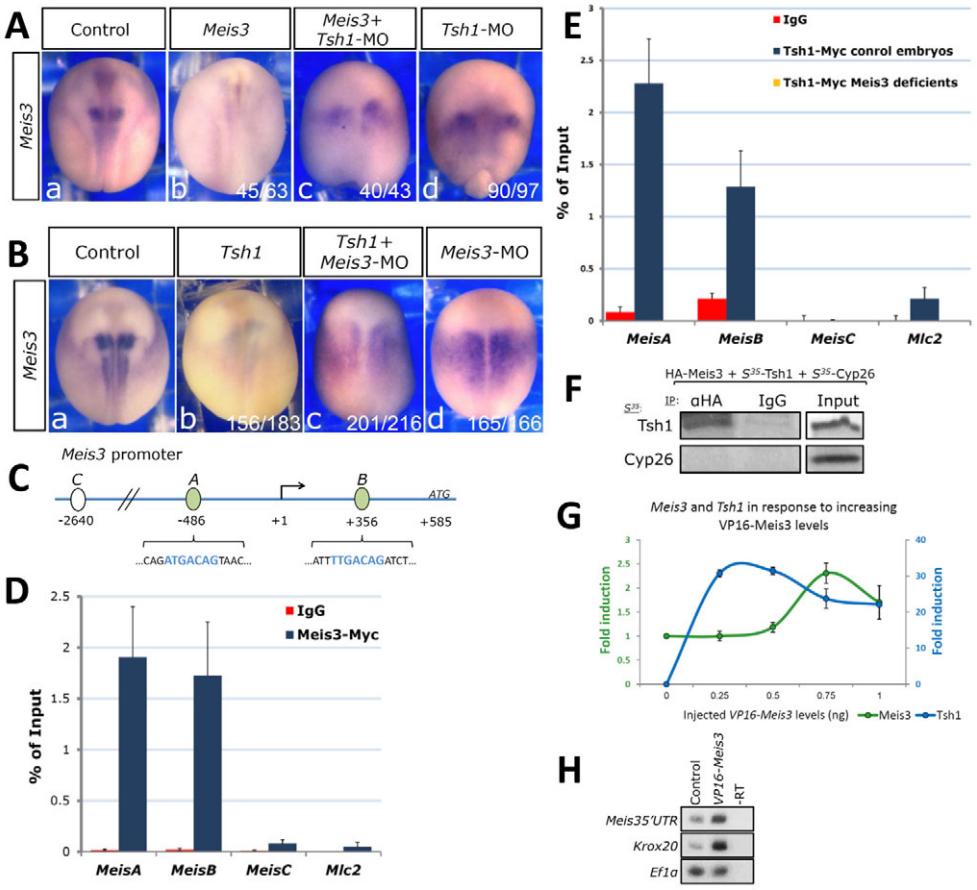

Fig. 4. Meis3 and Tsh1 act cooperatively on the *Meis3* promoter; recruited Tsh1 represses transcription. (**A**) *Meis3-5′UTR* expression analysis in mid-neurula embryos injected at the one-cell stage with *Meis3* mRNA (1 ng; b) or *Tsh1*-MO (5 pmol; a), or both (c). (**B**) *Meis3* expression in mid-neurula embryos injected at the one-cell stage with *Tsh1* mRNA (0.4 ng; b) or *Meis3*-MO (28 ng; d), or both (c). (**C**) A schematic representation of the *Meis3* proximal promoter region. Arrow indicates start of transcription; green ovals indicate two *Meis* consensus sites (A and B), indicated in light-blue text; white oval indicates ChIP-negative control site (C); numbers indicate positions relative to the transcription start site (+1); ATG (+585) is the translation initiation site. (**D**) ChIP-QPCR analysis on the *Meis3* promoter in *Meis3-Myc* injected embryos (0.8 ng) at mid-neurula stages. *MeisA* and *MeisB* are *Meis* consensus site amplicons, *MeisC* and *Mlc2* are negative control sites. IgG ChIP is a negative IP control. Pooled data from three independent experiments are represented as the percentage of input chromatin. Error bars are s.e.m. from three independent experiments. For amplicon primers, see supplementary material Table S2. (**E**) ChIP-QPCR analysis on the *Meis3* promoter in *Myc-Tsh1*-injected embryos (0.4 ng), either wild type or *Meis3*-MO (28 ng) co-injected, at mid-neurula stages. IgG-IP, *MeisC* and *Mlc2* are negative controls as in D. Pooled data from three independent experiments are represented as the percentage of input chromatin. Error bars are s.e.m. from three independent experiments. Tsh1-ChIP on *Meis3*-MO embryos (yellow) completely abolished the Tsh1-ChIP signal seen in wild-type embryos (dark blue). Tsh1 ChIP to both wild-type and *Meis3*-MO embryos were performed together in the same experiment and ChIP run; thus, Tsh1 ChIP on wild-type embryos is a positive control for Tsh1 ChIP on *Meis3*-MO embryos. (**F**) In vitro co-IP of Tsh1 and Meis3 proteins. In vitro synthesized HA-Meis3, S^{35}-Met-Tsh1 and S^{35}-Met-Cyp26 were mixed. HA-Meis3 IP was performed. IgG-IP and Cyp26 are a negative controls. (**G**) Kinetics of *Tsh1* and *Meis3* transcription in response to increasing levels of a forced Meis3 transcriptional activator. RT-PCR was performed on pools of 18 mid-neurula AC explants from *VP16-Meis3* mRNA-injected embryos (0.25-1 ng). Results were quantitated, normalized to the *Ef1α* control and plotted as fold change. Bars are s.e.m. from three independent experiments. –RT samples showed no DNA contamination. A '0' *x*-value is the non-injected controls, with a '1' *y*-value as a basal expression level. (**H**) RT-PCR to *Meis3-5′UTR* and *Krox20* in mid-neurula embryos injected with *VP16-Meis3* mRNA (250 pg). Robust *Krox20* expression controls for a strong Meis3 protein activity.

(Fig. 4D). As negative controls, we used a third region of *Meis3* promoter, which lacks a Meis-binding site (MeisC, –2640 bp; Fig. 4C), and a fragment of the *Mlc2* promoter. These control fragments were not enriched in the Meis3-IP sample; their levels did not exceed the IgG-IP control background levels (Fig. 4D). During sample preparation, we sheared the cross-linked DNA to fragments ≤1000 bp, with the vast majority ranging between 100 and 500 bp. We cannot completely eliminate the possibility of one site hitchhiking on the other, but our ChIP resolution suggests that both the *MeisA* and *MeisB* sites (~850 bp apart) are each bound by Meis3 protein. As *Meis3* is a direct-target gene of itself (Fig. 2D), Meis3 protein probably auto-activates or auto-represses its expression by binding these two consensus sites within its promoter.

Meis3 auto-activation occurs prior to *Tsh1* expression (Fig. 2D) and Tsh1 protein could be recruited to the *Meis3* promoter by Meis3 protein to repress gene expression. Thus, we determined by ChIP, whether Tsh1 also occupies the *MeisA* and *MeisB* sites. In *Myc-Tsh1* expressing embryos, both *MeisA* and *MeisB* sites were specifically bound in the Tsh1-IP sample and not in the IgG-IP

control (Fig. 4E). The control fragments were not enriched in the Tsh1-IP sample (Fig. 4E). Thus, Tsh1 binds the *Meis3* promoter via the two Meis sites. We determined whether Tsh1 occupancy is Meis3 dependent. Tsh1 ChIP analysis was performed as described, but in Meis3-morphant deficient embryos. Meis3 protein is absolutely required for Tsh1-*Meis3* promoter binding, as the Tsh1 ChIP signal on the *MeisA* and *MeisB* sites is abolished in Meis3-depleted embryos (Fig. 4E). The Tsh1 ChIP to both control and Meis3-deficient embryos were performed in the same experiment, and processed together, so that Tsh1-WT ChIP serves as a positive control for the Tsh1/Meis3-deficient ChIP. The experimental conditions were identical to Fig. 4B, thus coupling Tsh1 occupancy and function on the *Meis3* promoter. These results reveal a recruitment mechanism, in which Tsh1 protein requires Meis3 protein to bind the *Meis3* promoter.

Tsh1 binding the *Meis* promoter via Meis3 protein should require a physical interaction, and *Drosophila* Hth and Tsh proteins do interact (Bessa et al., 2002). We also detected specific physical interactions between the *Xenopus* Meis3 and Tsh1 proteins by co-IP in vitro (Fig. 4F). We used the Cyp26 protein as a negative control; *Cyp26* and *Meis3* expression do not overlap in the embryo, and are not predicted to physically interact (Fig. 4F). Thus, Meis3 and Tsh1 proteins probably physically interact to repress *Meis3* promoter transcription.

To verify that Tsh1 recruitment provides repressor function, we used a forced transcriptional-activator Meis3, VP16-Meis3 (Dibner et al., 2001). We monitored *Meis3* and *Tsh1* expression in response to increasing levels of ectopic VP16-Meis3 protein in AC explants (Fig. 4G). VP16-Meis3 strongly induces *Tsh1* expression (Fig. 4G), but is unable to repress *Meis3* expression. In contrast to the tenfold decrease in *Meis3* expression seen in AC explants expressing wild-type Meis3 protein (Fig. 3E), VP16-Meis3 induces a two-fold expression increase (Fig. 4G). This effect was also observed in vivo. VP16-Meis3 strongly induces *Meis3* and *Krox20* expression (Fig. 4H). Increased *Krox20* expression is the typical readout for strong wild-type Meis3 activity, which consistently downregulates endogenous *Meis3* expression (Fig. 2Ab). Unlike the wild-type Meis3 protein, VP16-Meis3 seems refractory to Wnt3a/Meis3/Tsh1 repression. When Tsh1 activity is overridden in the transcription complex on the *Meis3* promoter, there is no repression.

Meis3 plays a dual-role in hindbrain development and the Wnt3a/Meis3/Tsh1 circuit acts to promote neuron differentiation

We addressed the physiological role of *Meis3* suppression by the Wnt3a/Meis3/Tsh1 circuit. Whereas Meis3 is necessary for specification of primary neurons, strong Meis3 activity that induces hindbrain, typically inhibits terminal primary neuron differentiation (Gutkovich et al., 2010). Meis3 could play a dual role in hindbrain development: first, inducing cell types within the hindbrain, but later maintaining these cells in a proliferating progenitor state and preventing further differentiation. If so, Meis3 downregulation could stop proliferation, allow cell cycle exit and enhance differentiation. Indeed, in *Drosophila* eye and vertebrate retinal neuron development, Meis proteins induce eye/neuronal fate and proliferation, but their downregulation enables differentiation (Bessa et al., 2002; Bessa et al., 2008; Heine et al., 2008). Our observations that mid-neurula induced THVGR activity repressed *Meis3* expression without perturbing hindbrain marker expression (Fig. 1Bf,j), whereas neural-specific Wnt3a-deficiency modulated *n-Tub* expression in explants (Fig. 1Cd-f), support a later role for this Wnt3a/Meis3/Tsh1 circuit in primary neuron differentiation.

To address this issue, three experimental strategies were used to mis-express Meis3 protein at mid-late neurula stages, when it should be endogenously repressed. An inducible Meis3 (Meis3-GR) was overexpressed, and activated only prior to mid-neurula stages. VP16-Meis3 was also overexpressed; VP16-Meis3 is refractory to Wnt3a/Meis3/Tsh1 repression and constitutively upregulates *Meis3* expression (Fig. 4G,H). Finally, we used *Tsh1*-deficient embryos, in which endogenous *Meis3* expression is never repressed (Fig. 3Cc, Fig. 4Ad). In *Xenopus*, early neural progenitors express the *Iroquois 3* (*Iro3*) gene (Bellefroid et al., 1998; Gomez-Skarmeta et al., 1998). *Iro3* expression is followed by *Ngnr1* expression, which induces *NeuroD* expression and promotes primary neuron differentiation as marked by *n-Tub* expression (Sasai, 1998). Ngnr1 simultaneously represses *Iro3* expression, thus expression of *Iro3* in neural progenitors and *n-Tub* in fully differentiated primary neurons is mutually exclusive (Bellefroid et al., 1998). We examined *Meis3-GR*, *VP16-Meis3*-overexpressing and Tsh1-deficient embryos for *Iro3* versus *n-Tub* expression levels. Their proliferative state was determined by phospho-Histone H3 (PH3) immunostaining (Fig. 5A). For PH3 analysis, we used stacked images of multiple focal planes in cleared neural tubes, to allow for efficient visualization of proliferating cells. Meis3-GR was activated at mid-neurula stage; unactivated Meis3-GR had very weak activity in 15% of the embryos, whereas 85% developed normally (Fig. 5Ae-g).

All three *Meis3* mis-expressing strategies cause expanded *Iro3* expression, repression of *n-Tub* expression, and a marked increase in proliferating neural tube cells (Fig. 5Ah-p). Similar to *Meis3* in Tsh1-deficient embryos (Fig. 3Cc, Fig. 4Ad), *Iro3* expression is also expanded to its broader early-neurula stage pattern (Fig. 5An, inset). Furthermore, embryos injected into one blastomere at the two-cell stage with *VP16-Meis3* consistently expressed ectopic levels of *Iro3* and *Sox3*. *Sox3* specifically marks proliferating neural progenitors and not *n-Tub*-expressing primary neurons; like *Iro3* and *n-Tub* expression, *Sox3* and *n-Tub* expression are mutually exclusive (Bourguignon et al., 1998; Hardcastle and Papalopulu, 2000; Bonev et al., 2011). Double in situ hybridization shows that ectopic *Iro3* expression is restricted to *Sox3* expanded zones of expression on the injected-side (supplementary material Fig. S5A). These results show that, at neurula stages, Meis3 maintains the proliferative progenitor state of neurons, preventing their terminal differentiation. This later Meis3 activity is uncoupled from its earlier caudalizing activity (supplementary material Fig. S5B).

Reciprocally, we injected embryos with low concentrations of the *Meis3*-MO. This low *Meis3*-MO concentration causes a moderate reduction of Meis3 protein levels (Fig. 5Ay), resulting in a hypomorph (*Meis3*-MO^{Hypo}) phenotype. *Meis3*-MO^{Hypo} embryos could unmask the later effects of Meis3 protein depletion, without severely compromising its early functions in hindbrain formation, mimicking Meis3 reduction by the Wnt3a/Meis3/Tsh1 circuit. In *Meis3* hypomorphants, *Iro3* expression is unaffected or moderately decreased (Fig. 5Aq,t). Expression of *n-Tub* is expanded specifically in the hindbrain region, with ectopic neuron differentiation foci (Fig. 5Ab,r,u,v), which are also observed in the enlarged hindbrain-derived trigemimal neuron (Fig. 5Av,x). Proliferation is also reduced in *Meis3*-MO^{Hypo} embryos (Fig. 5As). This moderate decrease in Meis3 protein levels permits more cell cycle exit of neuron progenitors, enhancing differentiation. We used the VP16-Meis3 tool to analyze the transcriptional profile of Meis3-maintained neural progenitors. These cells fail to express the pro-neural marker genes *Ngnr1*, *Myt1*, *NeuroD* and *n-Tub*, while expressing high levels of *Iro3* (Fig. 5B), thus Meis3 maintains early *Iro3*+

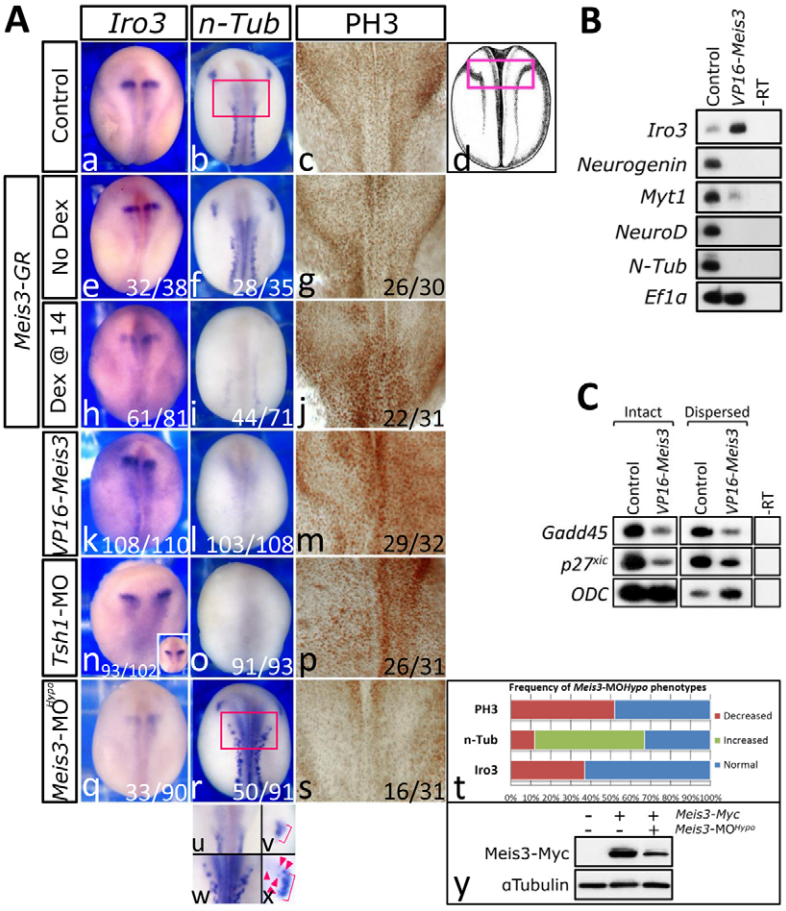

Fig. 5. Meis3 induces proliferative *Iro3*$^{+}$ neural progenitors and inhibits their terminal differentiation. (**A**) Embryos were injected at the one-cell stage with *Meis3-GR* (250 pg; e-j), or *VP16-Meis3* (250 pg; k-m) mRNAs, or *Tsh1*-MO (4 pmol; n-p) or *Meis3*-MO^{Hypo} (5 ng; q-s). Meis3-GR embryos were activated by 1 μM Dex at neurula stage 14, or kept untreated as controls. *Iro3* and *n-Tub* expression was examined at neurula stages. The inset (n) shows *Iro3* expression in early-stage wild-type embryos. u and w are magnifications of the hindbrain region (pink rectangle) of b and r, respectively. v and x show the trigeminal neuron of wild-type and *Meis3*-MO^{Hypo} embryos. Brackets and arrowheads indicate trigeminal expansion and ectopic differentiated foci, respectively. Cell proliferation was also assayed. Stacked images of 25 focal planes of cleared PH3-immunostained whole neural tubes are shown. Images are enlargements of the hindbrain region (pink rectangle in d). (t) *Meis3*-MO^{Hypo} phenotype frequency is shown. (y) Embryos were injected with *Meis3-Myc* (50 pg) and/or *Meis3*-MO^{Hypo} and western analysis at mid-neurula stages shows a moderate decrease in Meis3-Myc protein levels. (**B**) Transcriptional profiling of VP16-Meis3 neurons. RT-PCR to neural-specific developmental markers in mid-neurula embryos injected at the one-cell stage with *VP16-Meis3* (250 pg) mRNA. (**C**) Meis3 represses *p27Xic1* and *Gadd45γ* expression cell-autonomously. RT-PCR to *p27Xic1* and *Gadd45γ* in mid-neurula stage intact or dispersed AC explants from embryos injected with *VP16-Meis3* mRNA (0.8 ng).

proliferating neural progenitors that cannot differentiate. Further supporting a role for Meis3 protein as a cell-cycle regulator, ectopic VP16-Meis3 downregulated expression of the neural cell-cycle inhibitors *p27Xic1* and *Gadd45γ*, the activities of which are required for primary neuron differentiation (Vernon et al., 2003; de la Calle-Mustienes, 2003). VP16-Meis3 represses their expression cell autonomously, in both dissociated and intact AC explants (Fig. 5C). In the developing neural plate, the Wnt3a/Meis3/Tsh1 circuit is required to downregulate *Meis3* expression at the appropriate stage to promote neuron differentiation, presumably after a crucial mass of progenitors has formed. Tsh1 loss-of-function also perturbs neural tube closure, resulting in an early-like open neural plate (Fig. 3Cc, Fig. 4Ad, Fig. 5Ao,p). As Tsh1 loss of function causes an early-like upregulated expression of *Meis3* and *Iro3*, a stalling of primary neurons in a proliferative progenitor state, and an open neural plate morphology, we conclude that Tsh1 acts as a neural tissue maturation coordinating factor.

DISCUSSION

This study reveals a novel genetic circuit of Wnt3a, Meis3 and Tsh1 proteins that orchestrates downregulation of *Meis3* expression, restricting hindbrain induction and shifting neuronal progenitors to differentiation (Fig. 6A,C). We showed that early Wnt3a activates *Meis3* gene expression directly, as well as indirectly via Meis3 auto-induction. At later stages, high Meis3 protein levels activate *Tsh1* gene expression, leading to Tsh1 and Meis3 co-binding on the *Meis3* promoter (Fig. 6B). These delicate checks and balances between Wnt3a, Meis3 and Tsh1 protein activities are crucial for proper cell fate decisions in the maturing neural plate.

Tsh1 loss of function causes a compound phenotype. First, primary neurons remain in their proliferating progenitor state, failing to differentiate. Next, the neural transcription factors Meis3 and Iro3, maintain their early broad expression patterns, and are not downregulated to their later confined patterns. Finally, morphological cellular convergent extension (CE) movements required for proper neural tube closure are inhibited. CE movements are controlled by the Wnt planar cell polarity (PCP) pathway (Tissir and Goffinet, 2010). CE and active PCP are incompatible with cycling cells (Ciruna et al., 2006; Devenport et al., 2011); therefore, Tsh1 could induce cell cycle arrest in the neural plate, permitting PCP activity that drives neural tube closure. Immature neural tissue transforms from an open field of proliferating neural progenitors to a closed neural tube of differentiating cells. Neural tissue lacking Tsh1 exhibits immature characteristics. Tsh1 protein acts as a maturation factor that coordinates cell cycle exit, primary neuron differentiation and distinct cell movements in the neural plate.

Meis proteins form transcription complexes with Pbx and Hox proteins to activate target genes (Sagerstrom, 2004; Moens and Selleri, 2006). In the zebrafish hindbrain, Pbx4 protein recruits the transcriptional repressors CBP and HDAC to chromatin. Meis3 protein competes with Pbx4 to reduce promoter accessibility of HDAC and CBP to activate transcription (Choe et al., 2009). This is consistent with Meis3 hindbrain function as a transcriptional activator (Dibner et al., 2001). Supporting a conserved role for Tsh family proteins in hindbrain development, a recent genetic study in zebrafish showed that Tshz3b protein negatively regulated hindbrain Hox paralogous 1-4 gene function (Erickson et al., 2011).

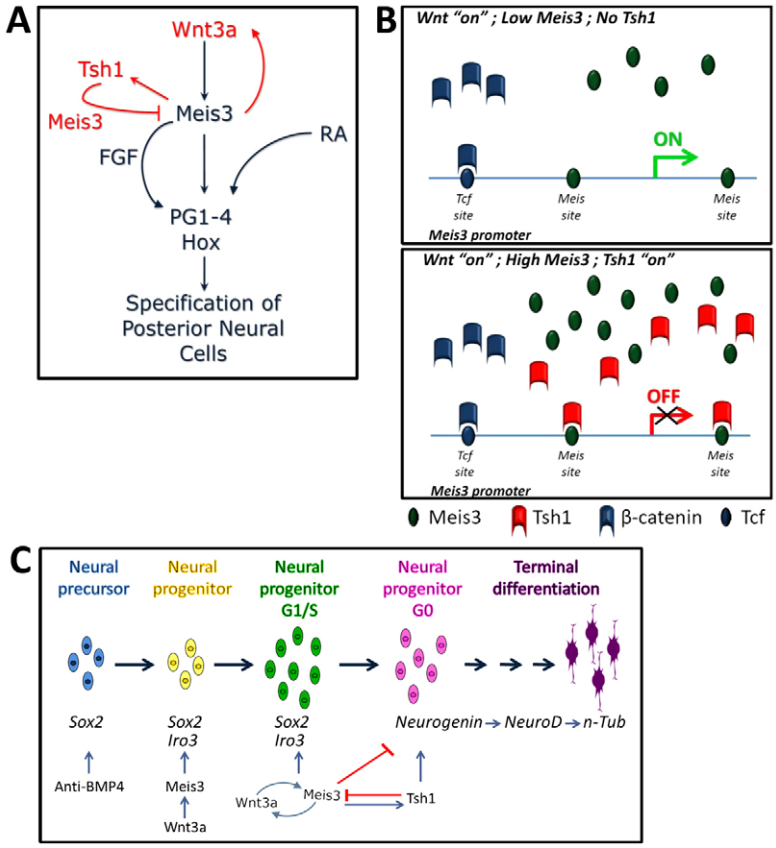

Fig. 6. A hindbrain repressive Wnt3a/Meis3/Tsh1 circuit promotes neuron differentiation. (**A**) The Wnt3a/Meis3/Tsh1 circuit (red arrows and blocks) represses the hindbrain developmental program (blue arrows). (**B**) Upper panel: β-catenin and Meis3 bind *Tcf* and *Meis* sites on the *Meis3* promoter to activate transcription. Lower panel: high Meis3 activity induces *Tsh1* expression. Tsh1 protein recruited to *Meis* sites represses *Meis3* transcription. (**C**) A model describing the Wnt3a/Meis3/Tsh1 circuits role in controlling gene expression and cell cycle at different stages of primary neuron development.

In a human neuroblastoma cell line, Tsh3 binds the FE65 adaptor protein recruiting HDAC to chromatin, suppressing *caspase 4* gene expression; in Alzheimer's brain postmortem samples, reduced *Tsh3*/*FE65* gene expression triggered an increase in caspase 4 levels, suggesting a causative role in disease progression (Kajiwara et al., 2009). Tsh3 also recruited repressive SWI/SNF proteins to chromatin in cultured myoblasts (Faralli et al., 2011). These studies support our observation of joint Meis3/Tsh1 repression of the *Meis3* promoter in the vertebrate hindbrain. Meis3 probably prevents HDAC recruitment, promoting *Meis3* transcription; later, Meis3-recruited Tsh1 directs transcriptional repression components to the complex. The *Meis3* promoter undergoes rapid stage-dependent changes in chromatin dynamics to modulate its expression; this flexibility allows fine-tuned regulation of neural cell fate decisions.

β-Catenin shuttles proteins into the nucleus (Fagotto et al., 1998) and *Xenopus* Tsh3 and *Drosophila* Tsh proteins undergo nuclear translocation via physical interaction with β-catenin (Gallet et al., 1998; Gallet et al., 1999; Onai et al., 2007). This challenges our observation that Tsh proteins inhibit Wnt/β-catenin activity. However, the coupled import of Tsh and β-catenin could serve as a potent cell-sensing mechanism, suggesting that Tsh nuclear shuttling occurs only under Wnt-activated conditions, when β-catenin enters the nucleus, ensuring Tsh-mediated restriction of *Meis3* expression in the appropriate time and place. High cellular Meis3 levels are prerequisite for *Tsh1* expression. This regulatory mechanism triggers Tsh1 inhibitory activity exclusively in cells where Meis3/Wnt/β-catenin neural caudalizing activity is high, thus explaining why early Wnt/β-catenin activity induces *Meis3* expression, but later suppresses it. This novel mechanism of Wnt modulation induces expression of a second protein, Tsh1, which then piggy-backs onto β-catenin to the nucleus to modify the transcriptional response of the pathway.

Wnt acts at multiple stages in the induction, proliferation and differentiation of neurons (Megason and McMahon, 2002; Amoyel et al., 2005; Nordstrom et al., 2006; Elkouby et al., 2010). We suggest a mechanism in which Meis3-Tsh1 interplay explain this signaling integration. At gastrula stages, Wnt/β-catenin activates *Meis3* expression, which induces primary neuron precursors. At neurula stages, Wnt/β-catenin and Meis3 activities are both required to induce *Tsh1* expression, subsequently repressing *Meis3* expression, shifting progenitor cells from a proliferative determined state to terminal differentiation.

Meis3 protein has a dual role in the developing hindbrain. Although Meis3 is required for early hindbrain formation, including primary neuron induction (Gutkovich et al., 2010), we have unmasked a later role controlling primary neuron differentiation. Meis3 protein maintains early-induced primary neurons in a proliferative progenitor state, preventing differentiation (Fig. 6C). This dual-role was also shown in *Drosophila* eye and vertebrate retinal development. Meis proteins first induce eye/retinal neuron cell fate and proliferation, but then undergo downregulation enabling differentiation (Bessa et al., 2002; Bessa et al., 2008; Heine et al., 2008). In the vertebrate retina, Meis1 induces *cyclinD1* expression that acts in G1-S transition to promote proliferation (Bessa et al., 2008; Heine et al., 2008). Meis1 is also mitogenic in BM hematopoietic cells, directly activating the *cyclinD3* promoter, driving G1-S transition (Argiropoulos et al., 2010). Some cyclins and cdks overlap with hindbrain *Meis3* expression (Vernon and Philpott, 2003). Overexpression of the G1/S cyclinA2-cdk2 pair induces

proliferation and inhibits neuron differentiation in *Xenopus* (Richard-Parpaillon et al., 2004). It would be interesting to examine the potential regulation of hindbrain cyclin/cdk expression by Meis3. Interestingly, we show that Meis3 strongly downregulates *p27Xic1* and *Gadd45γ* expression. These cell cycle inhibitors promote cell cycle exit required for primary neuron differentiation (Vernon et al., 2003; de la Calle-Mustienes, 2003). Plant TALE homologues exhibit this duality during compound leaf development (Shani et al., 2009). Our work supports this dual developmental strategy for Meis/KNOX proteins as a general evolutionary trait.

Meis3-induced progenitors are stalled as *Iro3*+ neurons, consistent with our findings that Meis3 induces primary neurons upstream of Ngnr1 activity (Gutkovich et al., 2010). Furthermore, Ngnr1-induced primary neuron differentiation in Meis3-depleted embryos was much stronger than in wild-type embryos (Gutkovich et al., 2010), suggesting that in order to maintain the *Iro3*+ state, Meis3 could potentially inhibit neuron differentiation by repressing *p27Xic1* and *Gadd45γ* gene expression. Meis3 inhibition released the unregulated full capacity of Ngnr1 neuron-inducing activity. In Meis3-induced progenitors, upregulated cell cycle activators and downregulated cell cycle inhibitors could prevent cell cycle exit, regardless of pro-neural gene expression. Such uncoupled regulation was shown for Meis1 in the retina (Bessa et al., 2008; Heine et al., 2008). *Iro3* expression is strongly induced by Meis3, and Iro protein positively regulates pro-neural gene expression (Bellfroid et al., 1998; Gomez-Skarmeta et al., 1998). Iro3 neural progenitor maintenance was suggested to require interactions with other factors, and its downregulation was required for neuron differentiation (Bellfroid et al., 1998). Hth, Iro and Tsh proteins form differential transcriptional complexes in *Drosophila* (Pichaud and Casares, 2000; Bessa et al., 2002), and their expression overlaps in the vertebrate hindbrain. Expression of *Iro3*, cyclin genes, *cdk* inhibitors and pro-neural genes could be differentially regulated by distinct Meis3/Iro3/Tsh1 complexes. Indeed, Meis3-expressing/Tsh1-deficient progenitors do not express pro-neural genes but show strong *Iro3* expression. We show that Tsh1 suppresses *Iro3* expression and activity, suggesting a similar Tsh1 repressive recruitment to a potential Meis3-Iro3 complex.

Both Meis proteins and Wnt/β-catenin signaling act as acute myeloid leukemia (AML)-promoting factors (Eklund, 2007; Mikesch et al., 2007). Wnt pathway components and Meis proteins are overexpressed and activated in AML cells (Eklund, 2007; Mikesch et al., 2007). Analogous to the dual-role of Meis3, Meis1 and Meis3 proteins induce both AML transformation and malignant progression acceleration, which are the rate limiting regulators of AML (Thorsteinsdottir et al., 2001; Wang et al., 2006; Wong et al., 2007). In AML cells, *Flt3* is a Meis1 direct-target gene that induces Wnt/β-catenin activity (Wang et al., 2006; Mikesch et al., 2007). Recently, Tsh proteins were implicated as tumor suppressors in breast and prostate cancer (Yamamoto et al., 2011). Perhaps *Tsh* gene expression is downregulated in AML, which triggers de-regulated Meis and Wnt protein activities. Tsh transcriptional repressor function was suggested to regulate target genes in Alzheimer's disease progression (Kajiwara et al., 2009). We show that Meis3 and Tsh1 protein interplay converges on *Meis*3 gene expression to coordinate the induction, proliferation and differentiation of developing neurons. Further investigation will determine whether other Wnt/Meis/Tsh genetic circuits have analogous roles in regulating diverse developmental processes, as well as cancer and neurodegenerative disease.

Acknowledgements
We thank Drs J. Kashef, D. Wedlich and J. L. Gomez-Skarmata for plasmids, Dr S. Blythe for ChIP advice, and Dr D. Geerts for bioinformatics assistance.

Funding
D.F. was supported by a grant from the Israel Science Foundation (658/09).

Competing interests statement
The authors declare no competing financial interests.

Supplementary material
Supplementary material available online at
http://dev.biologists.org/lookup/suppl/doi:10.1242/dev.072934/-/DC1

References
Aamar, E. and Frank, D. (2004). Xenopus Meis3 protein forms a hindbrain-inducing center by activating FGF/MAP kinase and PCP pathways. *Development* **131**, 153-163.
Amoyel, M., Cheng, Y. C., Jiang, Y. J. and Wilkinson, D. G. (2005). Wnt1 regulates neurogenesis and mediates lateral inhibition of boundary cell specification in the zebrafish hindbrain. *Development* **132**, 775-785.
Argiropoulos, B., Yung, E., Xiang, P., Lo, C. Y., Kuchenbauer, F., Palmqvist, L., Reindl, C., Heuser, M., Sekulovic, S., Rosten, P. et al. (2010). Linkage of the potent leukemogenic activity of Meis1 to cell-cycle entry and transcriptional regulation of cyclin D3. *Blood* **115**, 4071-4082.
Bellefroid, E. J., Kobbe, A., Gruss, P., Pieler, T., Gurdon, J. B. and Papalopulu, N. (1998). Xiro3 encodes a Xenopus homolog of the Drosophila Iroquois genes and functions in neural specification. *EMBO J.* **17**, 191-203.
Bessa, J., Gebelein, B., Pichaud, F., Casares, F. and Mann, R. S. (2002). Combinatorial control of Drosophila eye development by eyeless, homothorax, and teashirt. *Genes Dev.* **16**, 2415-2427.
Bessa, J., Tavares, M. J., Santos, J., Kikuta, H., Laplante, M., Becker, T. S., Gomez-Skarmeta, J. L. and Casares, F. (2008). meis1 regulates cyclin D1 and c-myc expression, and controls the proliferation of the multipotent cells in the early developing zebrafish eye. *Development* **135**, 799-803.
Blythe, S. A., Reid, C. D., Kessler, D. S. and Klein, P. S. (2009). Chromatin immunoprecipitation in early Xenopus laevis embryos. *Dev. Dyn.* **238**, 1422-1432.
Bonev, B., Pisco, A. and Papalopulu, N. (2011). MicroRNA-9 reveals regional diversity of neural progenitors along the anterior-posterior axis. *Dev. Cell* **20**, 19-32.
Bonstein, L., Elias, S. and Frank, D. (1998). Paraxial-fated mesoderm is required for neural crest induction in Xenopus embryos. *Dev. Biol.* **193**, 156-168.
Bourguignon, C., Li, J. and Papalopulu, N. (1998). XBF-1, a winged helix transcription factor with dual activity, has a role in positioning neurogenesis in Xenopus competent ectoderm. *Development* **124**, 4889-4900.
Casares, F. and Mann, R. S. (2000). A dual role for homothorax in inhibiting wing blade development and specifying proximal wing identities in Drosophila. *Development* **127**, 1499-1508.
Choe, S. K., Lu, P., Nakamura, M., Lee, J. and Sagerstrom, C. G. (2009). Meis cofactors control HDAC and CBP accessibility at Hox-regulated promoters during zebrafish embryogenesis. *Dev. Cell* **17**, 561-567.
Ciruna, B., Jenny, A., Lee, D., Mlodzik, M. and Schier, A. F. (2006). Planar cell polarity signalling couples cell division and morphogenesis during neurulation. *Nature* **439**, 220-224.
de la Calle-Mustienes, E., Glavic, A., Modolell, J. and Gomez-Skarmeta, J. L. (2002). Xiro homeoproteins coordinate cell cycle exit and primary neuron formation by upregulating neuronal-fate repressors and downregulating the cell-cycle inhbitor XGadd-45-gamma. *Mech. Dev.* **119**, 69-80.
Devenport, D., Oristian, D., Heller, E. and Fuchs, E. (2011). Mitotic internalization of planar cell polarity proteins preserves tissue polarity. *Nat. Cell Biol.* **10**, 1257-1268
Dibner, C., Elias, S. and Frank, D. (2001). XMeis3 protein activity is required for proper hindbrain patterning in Xenopus laevis embryos. *Development* **128**, 3415-3426.
Dibner, C., Elias, S., Ofir, R., Souopgui, J., Kolm, P. J., Sive, H., Pieler, T. and Frank, D. (2004). The Meis3 protein and retinoid signaling interact to pattern the Xenopus hindbrain. *Dev. Biol.* **271**, 75-86.
Dorey, K. and Amaya, E. (2010). FGF signalling: diverse roles during early vertebrate embryogenesis. *Development* **137**, 3731-3742.
Eklund, E. A. (2007). The role of HOX genes in malignant myeloid disease. *Curr. Opin. Hematol.* **14**, 85-89.
Elkouby, Y. M. and Frank, D. (2010). Wnt/β-catenin signaling in vertebrate posterior neural development. In *Colloquium Series on Developmental Biology* (ed. D. S. Kessler), eBook 4. San Rafael, CA: Morgan & Claypool Life Sciences.
Elkouby, Y. M., Elias, S., Casey, E. S., Blythe, S. A., Tsabar, N., Klein, P. S., Root, H., Liu, K. J. and Frank, D. (2010). Mesodermal Wnt signaling organizes the neural plate via Meis3. *Development* **137**, 1531-1541.

Erickson, T., Pillay, L. M. and Waskiewicz, A. J. (2011). Zebrafish Tshz3b negatively regulates Hox function in the developing hindbrain. *Genesis* **49**, 725-742.
Fagotto, F., Gluck, U. and Gumbiner, B. M. (1998). Nuclear localization signal-independent and importin/karyopherin-independent nuclear import of beta-catenin. *Curr. Biol.* **8**, 181-190.
Faralli, H., Martin, E., Coré, N., Liu, Q. C., Filippi, P., Dilworth, F. J., Caubit, X. and Fasano, L. (2011). Teashirt-3, a novel regulator of muscle differentiation, associates with BRG1-associated factor 57 (BAF57) to inhibit myogenin gene expression. *J. Biol. Chem.* **286**, 23498-23510.
Fonar, Y., Gutkovich, Y. E., Root, H., Malyarova, A., Aamar, E., Golubovskaya, V. M., Elias, S., Elkouby, Y. M. and Frank, D. (2011). Focal adhesion kinase protein regulates Wnt3a gene expression to control cell fate specification in the developing neural plate. *Mol. Biol. Cell* **22**, 2409-2421.
Gallet, A., Erkner, A., Charroux, B., Fasano, L. and Kerridge, S. (1998). Trunk-specific modulation of wingless signalling in Drosophila by teashirt binding to armadillo. *Curr. Biol.* **8**, 893-902.
Gallet, A., Angelats, C., Erkner, A., Charroux, B., Fasano, L. and Kerridge, S. (1999). The C-terminal domain of armadillo binds to hypophosphorylated teashirt to modulate wingless signalling in Drosophila. *EMBO J.* **18**, 2208-2217.
Glinka, A., Wu, W., Delius, H., Monaghan, A. P., Blumenstock, C. and Niehrs, C. (1998). Dickkopf-1 is a member of a new family of secreted proteins and functions in head induction. *Nature* **391**, 357-362.
Gomez-Skarmeta, J. L., Glavic, A., de la Calle-Mustienes, E., Modolell, J. and Mayor, R. (1998). Xiro, a Xenopus homolog of the Drosophila Iroquois complex genes, controls development at the neural plate. *EMBO J.* **17**, 181-190.
Gutkovich, Y. E., Ofir, R., Elkouby, Y. M., Dibner, C., Gefen, A., Elias, S. and Frank, D. (2010). Xenopus Meis3 protein lies at a nexus downstream to Zic1 and Pax3 proteins, regulating multiple cell-fates during early nervous system development. *Dev. Biol.* **338**, 50-62.
Hardcastle, Z. and Papalopulu, N. (2000). Distinct effects of XBF-1 in regulating the cell cycle inhibitor p27(XIC1) and imparting neural fate. *Development* **127**, 1303-1314.
Harland, R. M. (1991). In situ hybridization: an improved whole-mount method for Xenopus embryos. *Methods Cell Biol.* **36**, 685-695.
Heine, P., Dohle, E., Bumsted-O'Brien, K., Engelkamp, D. and Schulte, D. (2008). Evidence for an evolutionary conserved role of homothorax/Meis1/2 during vertebrate retina development. *Development* **135**, 805-811.
Inbal, A., Halachmi, N., Dibner, C., Frank, D. and Salzberg, A. (2001). Genetic evidence for the transcriptional-activating function of Homothorax during adult fly development. *Development* **128**, 3405-3413.
Kajiwara, Y., Akram, A., Katsel, P., Haroutunian, V., Schmeidler, J., Beecham, G., Haines, J. L., Pericak-Vance, M. A. and Buxbaum, J. D. (2009). FE65 binds Teashirt, inhibiting expression of the primate-specific caspase-4. *PLoS ONE* **4**, e5071.
Koebernick, K., Kashef, J., Pieler, T. and Wedlich, D. (2006). Xenopus Teashirt1 regulates posterior identity in brain and cranial neural crest. *Dev. Biol.* **298**, 312-326.
McGrew, L. L., Hoppler, S. and Moon, R. T. (1997). Wnt and FGF pathways cooperatively pattern anteroposterior neural ectoderm in Xenopus. *Mech. Dev.* **69**, 105-114.
Megason, S. G. and McMahon, A. P. (2002). A mitogen gradient of dorsal midline Wnts organizes growth in the CNS. *Development* **129**, 2087-2098.
Mikesch, J. H., Steffen, B., Berdel, W. E., Serve, H. and Muller-Tidow, C. (2007). The emerging role of Wnt signaling in the pathogenesis of acute myeloid leukemia. *Leukemia* **21**, 1638-1647.
Moens, C. B. and Selleri, L. (2006). Hox cofactors in vertebrate development. *Dev. Biol.* **291**, 193-206.
Nordstrom, U., Maier, E., Jessell, T. M. and Edlund, T. (2006). An early role for WNT signaling in specifying neural patterns of Cdx and Hox gene expression and motor neuron subtype identity. *PLoS Biol.* **4**, e252.
Onai, T., Matsuo-Takasaki, M., Inomata, H., Aramaki, T., Matsumura, M., Yakura, R., Sasai, N. and Sasai, Y. (2007). XTsh3 is an essential enhancing factor of canonical Wnt signaling in Xenopus axial determination. *EMBO J.* **26**, 2350-2360.
Pichaud, F. and Casares, F. (2000). Homothorax and iroquois-C genes are required for the establishment of territories within the developing eye disc. *Mech. Dev.* **96**, 15-25.
Re'em-Kalma, Y., Lamb, T. and Frank, D. (1995). Competition between noggin and bone morphogenetic protein 4 activities may regulate dorsalization during Xenopus development. *Proc. Natl. Acad. Sci. USA* **92**, 12141-12145.
Richard-Parpaillon, L., Cosgrove, R. A., Devine, C., Vernon, A. E. and Philpott, A. (2004). G1/S phase cyclin-dependent kinase overexpression perturbs early development and delays tissue-specific differentiation in Xenopus. *Development* **131**, 2577-2586.
Sagerstrom, C. G. (2004). PbX marks the spot. *Dev. Cell* **6**, 737-738.
Salzberg, A., Elias, S., Nachaliel, N., Bonstein, L., Henig, C. and Frank, D. (1999). A Meis family protein caudalizes neural cell fates in Xenopus. *Mech. Dev.* **80**, 3-13.
Sasai, Y. (1998). Identifying the missing links: genes that connect neural induction and primary neurogenesis in vertebrate embryos. *Neuron* **21**, 455-458.
Shani, E., Burko, Y., Ben-Yaakov, L., Berger, Y., Amsellem, Z., Goldshmidt, A., Sharon, E. and Ori, N. (2009). Stage-specific regulation of Solanum lycopersicum leaf maturation by class 1 KNOTTED1-LIKE HOMEOBOX proteins. *Plant Cell* **21**, 3078-3092.
Snir, M., Ofir, R., Elias, S. and Frank, D. (2006). Xenopus laevis POU91 protein, an Oct3/4 homologue, regulates competence transitions from mesoderm to neural cell fates. *EMBO J.* **25**, 3664-3674.
Thorsteinsdottir, U., Kroon, E., Jerome, L., Blasi, F. and Sauvageau, G. (2001). Defining roles for HOX and MEIS1 genes in induction of acute myeloid leukemia. *Mol. Cell. Biol.* **21**, 224-234.
Tissir, F. and Goffinet, A. M. (2010). Planar cell polarity signaling in neural development. *Curr. Opin. Neurobiol.* **20**, 572-577.
Vernon, A. E. and Philpott, A. (2003). The developmental expression of cell cycle regulators in Xenopus laevis. *Gene Expr. Patterns* **3**, 179-192.
Vernon, A. E., Devine, C. and Philpott, A. (2003). The cdk inhbitory p27Xic1 is required for differentiation of primary neurones in Xenopus. *Development* **130**, 85-92.
Vlachakis, N., Choe, S. K. and Sagerstrom, C. G. (2001). Meis3 synergizes with Pbx4 and Hoxb1b in promoting hindbrain fates in the zebrafish. *Development* **128**, 1299-1312.
Waltzer, L., Vandel, L. and Bienz, M. (2001). Teashirt is required for transcriptional repression mediated by high Wingless levels. *EMBO J.* **20**, 137-145.
Wang, G. G., Pasillas, M. P. and Kamps, M. P. (2006). Persistent transactivation by meis1 replaces hox function in myeloid leukemogenesis models: evidence for co-occupancy of meis1-pbx and hox-pbx complexes on promoters of leukemia-associated genes. *Mol. Cell. Biol.* **26**, 3902-3916.
Waskiewicz, A. J., Rikhof, H. A., Hernandez, R. E. and Moens, C. B. (2001). Zebrafish Meis functions to stabilize Pbx proteins and regulate hindbrain patterning. *Development* **128**, 4139-4151.
White, R. J. and Schilling, T. F. (2008). How degrading: Cyp26s in hindbrain development. *Dev. Dyn.* **237**, 2775-2790.
Wong, P., Iwasaki, M., Somervaille, T. C., So, C. W. and Cleary, M. L. (2007). Meis1 is an essential and rate-limiting regulator of MLL leukemia stem cell potential. *Genes Dev.* **21**, 2762-2774.
Wu, J., Yang, J. and Klein, P. S. (2005). Neural crest induction by the canonical Wnt pathway can be dissociated from anterior-posterior neural patterning in Xenopus. *Dev. Biol.* **279**, 220-232.
Yamamoto, M., Cid, E., Bru, S. and Yamamoto, F. (2011). Rare and frequent promoter methylation, respectively, of TSHZ2 and 3 genes that are both downregulated in expression in breast and prostate cancers. *PLoS ONE* **6**, e17149.

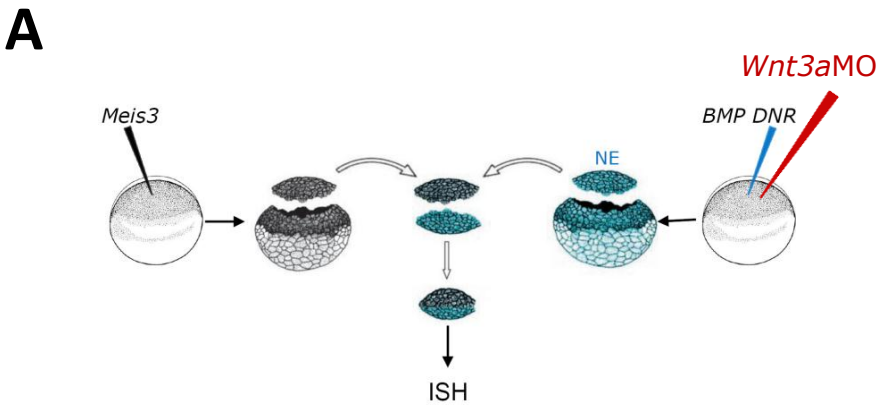
A
Wnt3aMO
Meis3
BMP DNR
NE
ISH

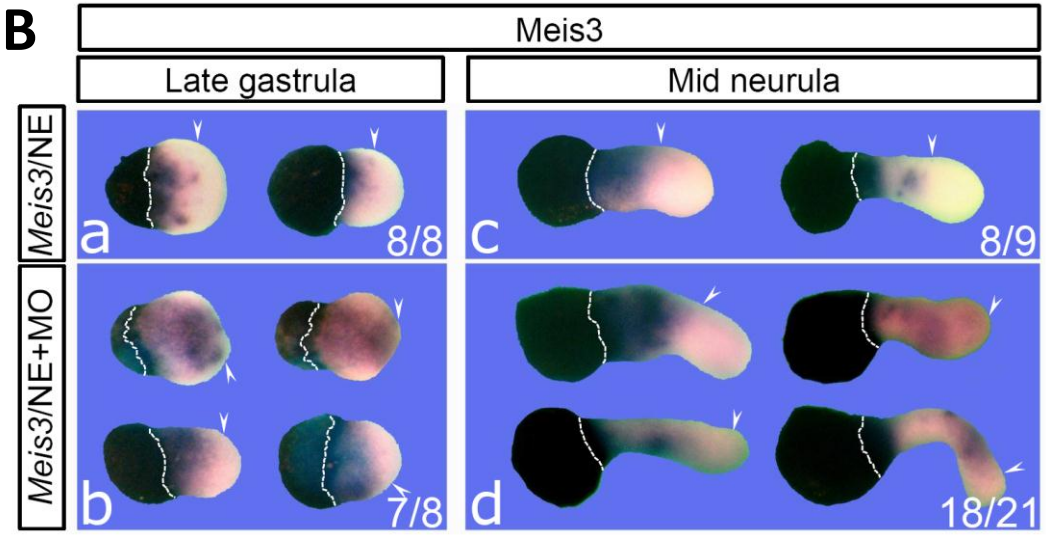
B
Meis3
Late gastrula
Mid neurula
Meis3/NE
Meis3/NE+MO
a
8/8
c
8/9
b
7/8
d
18/21

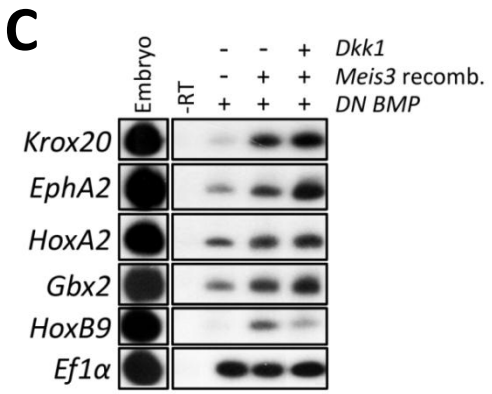
C
Embryo
-RT
Dkk1
Meis3 recomb.
DN BMP
Krox20
EphA2
HoxA2
Gbx2
HoxB9
Ef1α

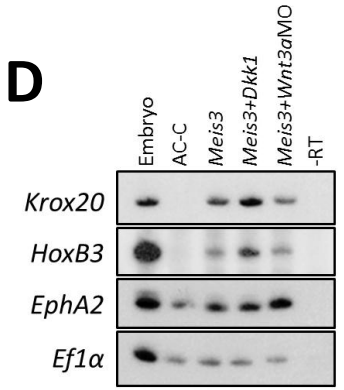
D
Embryo
AC-C
Meis3
Meis3+Dkk1
Meis3+Wnt3aMO
-RT
Krox20
HoxB3
EphA2
Ef1α

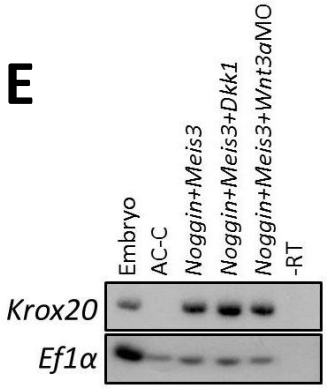
E
Embryo
AC-C
Noggin+Meis3
Noggin+Meis3+Dkk1
Noggin+Meis3+Wnt3aMO
-RT
Krox20
Ef1α

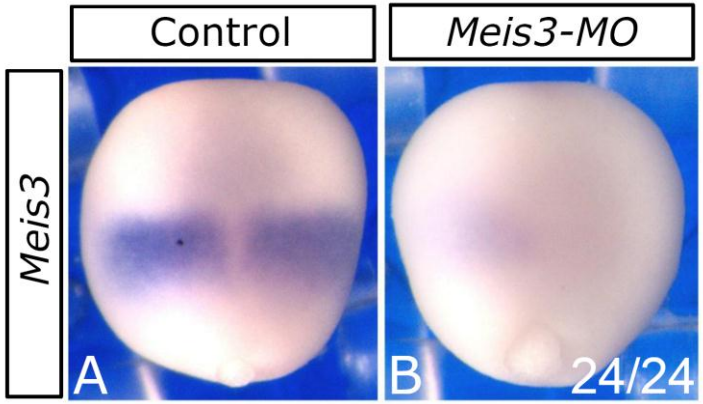
Control
Meis3-MO
Meis3
A
B
24/24

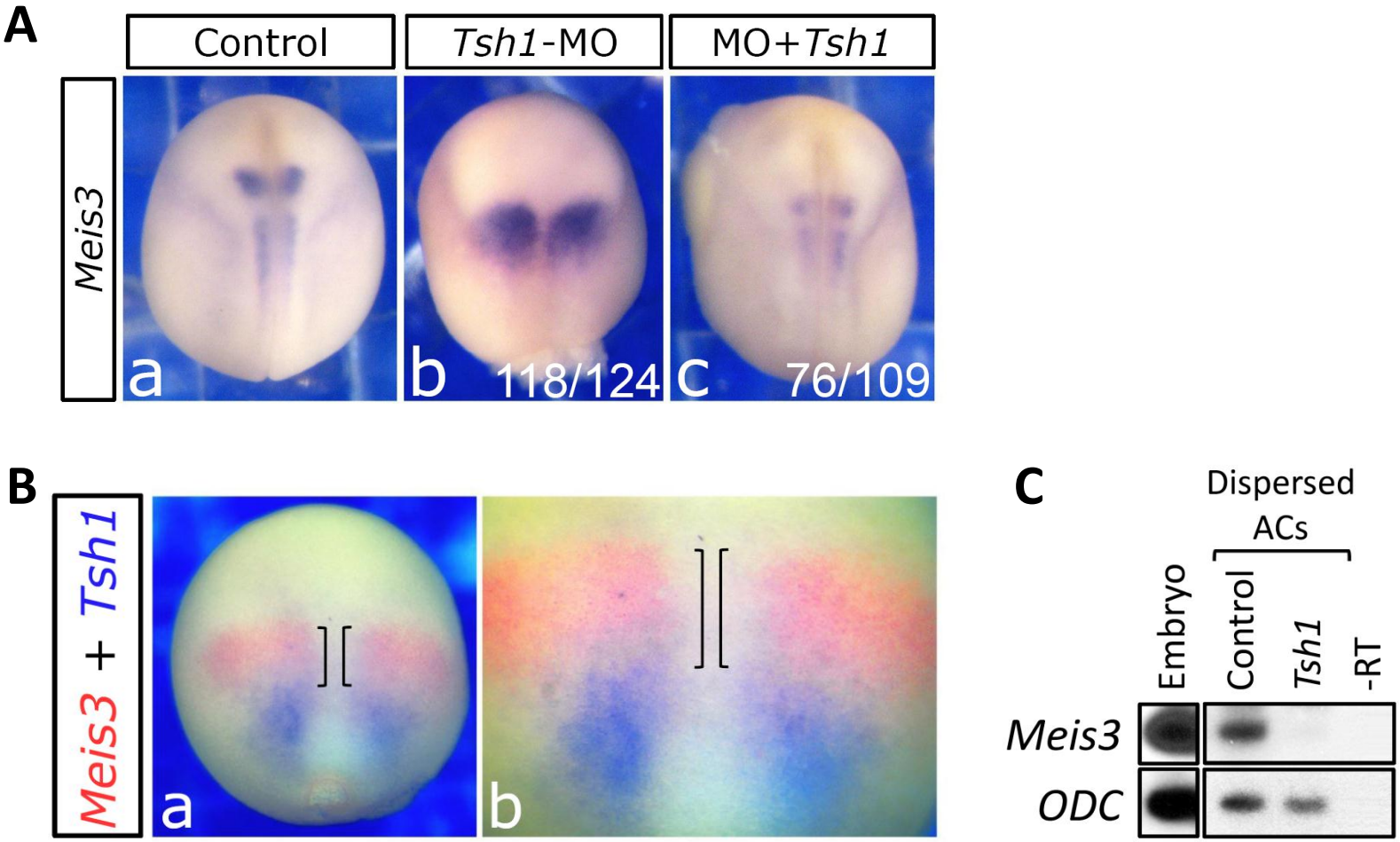
A
Control
Tsh1-MO
MO+Tsh1
Meis3
a
b
118/124
c
76/109
B
Meis3 + Tsh1
a
b
C
Dispersed ACs
Embryo
Control
Tsh1
-RT
Meis3
ODC

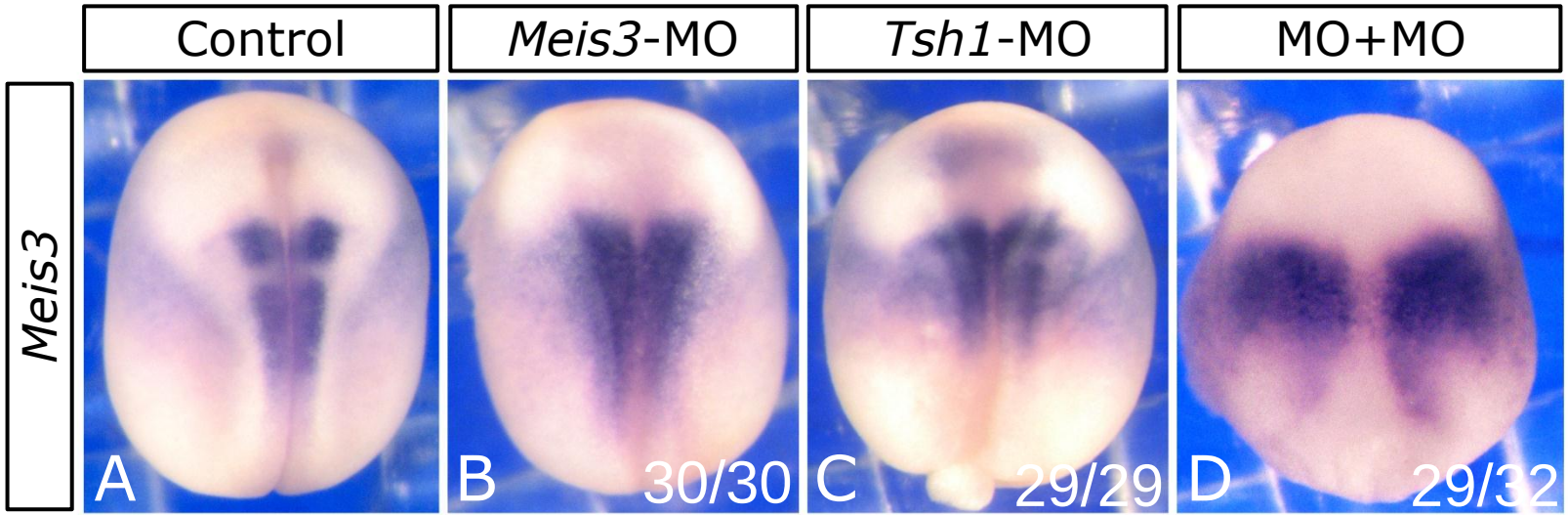
Control
Meis3-MO
Tsh1-MO
MO+MO
Meis3
A
B
30/30
C
29/29
D
29/32

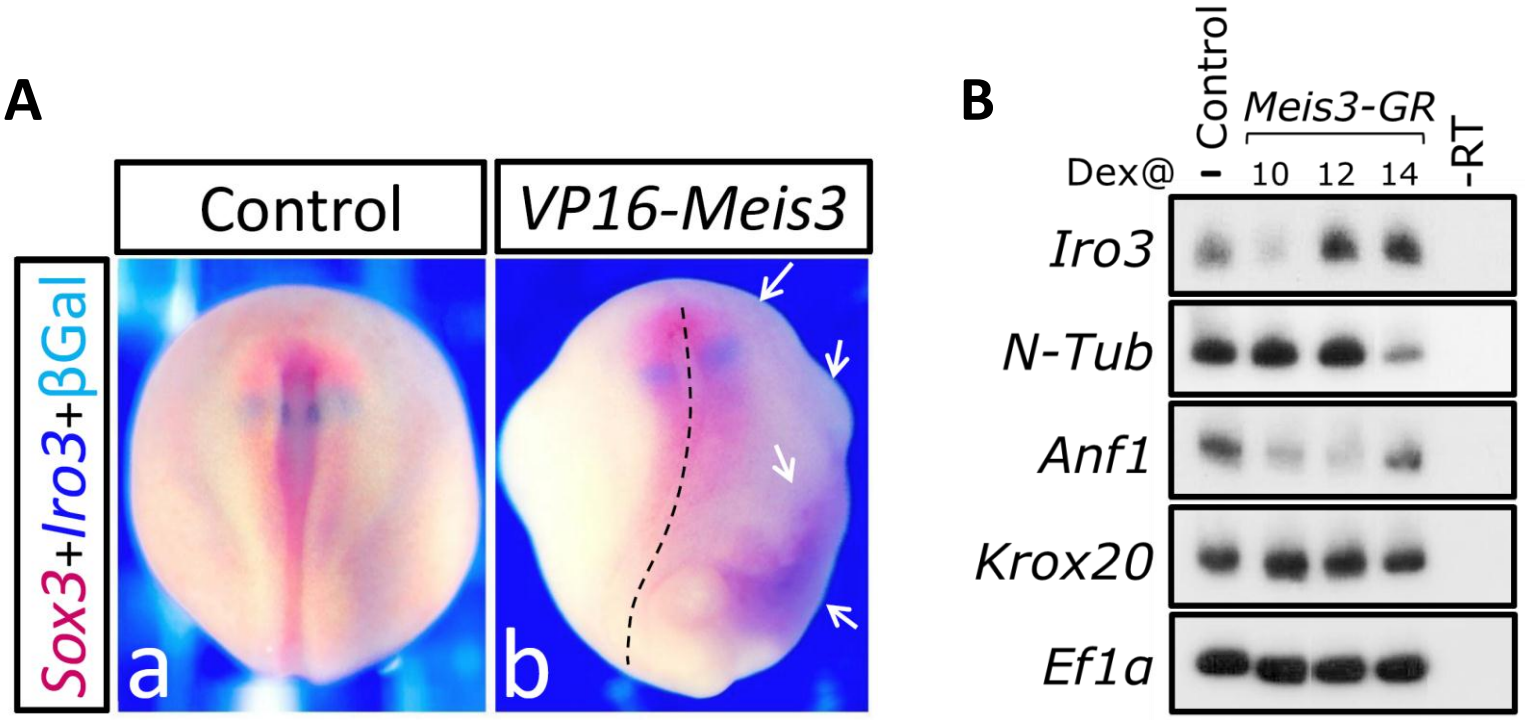
A
Control
VP16-Meis3
Sox3+Iro3+βGal
a
b
B
Control
Meis3-GR
Dex@
-
10
12
14
-RT
Iro3
N-Tub
Anf1
Krox20
Ef1a

Table S1. ChIP qPCR conditions

Amplicon	Oligo sequence (5′ to 3′)	Primer (mM)	Threshold
MeisA	For: CCATAGCCTACAGAGCGGA Rev: GTTACTGTCATCTGCCAAG	300	1000
MeisB	For: GACTGGAGCACCAACAGAGG Rev: CCATCAAGGTTGCAAGATCTGTC	300	100
MeisC	For: CAGGTCATGGAACTCCGAG Rev: GAGTAGTGATGTCATTTCTGTCAC	100	260
Mlc2	(Blythe et al., 2009)	300	1400

Table S2. sqRT-PCR primer sets

Gene	Primer sequences (5′ to 3′)
EF1a	Gutkovich et al., 2010
Krox20	Gutkovich et al., 2010
HoxB3	Gutkovich et al., 2010
HoxB9	Gutkovich et al., 2010
Meis3	Gutkovich et al., 2010
Ngnr1	Gutkovich et al., 2010
NeuroD	Gutkovich et al., 2010
n-Tub	Gutkovich et al., 2010
Anf1	Fonar et al., 2011
EphA2	Fonar et al., 2011
ODC	Elkouby et al., 2010
Iro3	for: CAACGGAGGTCACAAGATCA rev: AACCATACGAACTCAGCTGC
Myt1	for: CTTATGGTAGAAGAGGCGTG rev: CATCATCTGATCTGACCTCC
Tsh1	for: TGAGTGAGGCGACTGGTTCTACA rev: GCAGCCTGGTGCCAATCATAC
Meis3-5'UTR	for: GGAGACTAGAGCATGGAG rev: GTGTTGGTTCTGTCTGGA
Gadd45γ	for: GTGAGGCTGAACGACACAGA rev: CATAGACTTTGCGGCTTTCC
p27Xic1	for: GTGGCACCCCTCTTAAGGGC rev: TTCCAGTGGGCACAATAGGT